

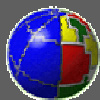


# MODELING INSTANTANEOUS DYNAMIC TRIGGERING IN A 3 - D FAULT SYSTEM: THE CASE OF AN EARLY AND REMOTE AFTERSHOCK IN THE JUNE 2000 SOUTH ICELAND SEISMIC SEQUENCE

Andrea Bizzarri <sup>1</sup>, Maria Elina Belardinelli <sup>2</sup>

<sup>1</sup> Istituto Nazionale di Geofisica e Vulcanologia – Sezione di Bologna

<sup>2</sup> Università degli Studi di Bologna – Dipartimento di Fisica



*April 18 2007*

# Motivations and Goals

- Remote triggering is a case of dynamic triggering occurring at distances larger than the dimension of the causative fault;
- Since the  $M_w$  7.7 1992 Landers EQ only a few examples of remote triggering have been observed; we consider the early events in Reykjanes Peninsula on June 17, 2000;

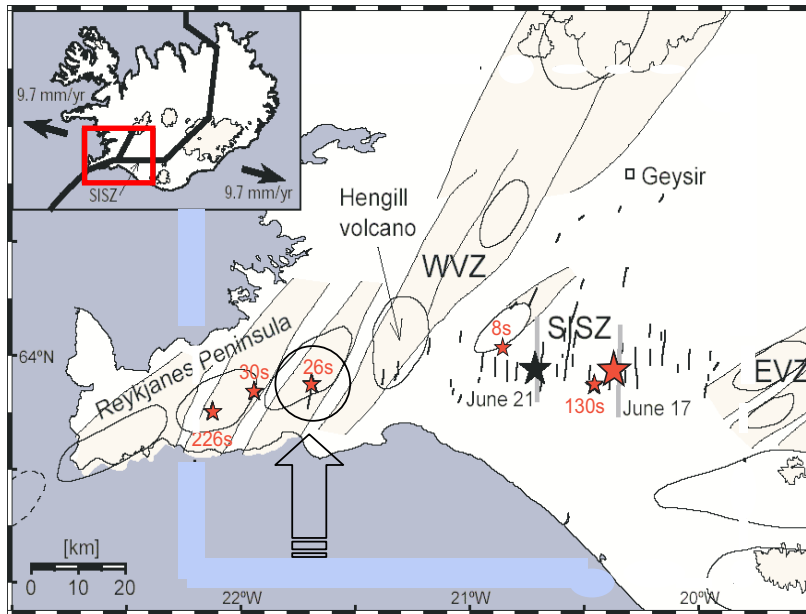
➡ We study the instantaneous remote triggering of a fault of finite extension, considering a realistic 3-D fault model, including heterogeneities in the crustal profile and in the fault rheology;

➡ We generalize the conclusions obtained in a previous paper on the basis of a simple 1-D spring-slider analog system;

➡ We study the response of the triggered fault as depending on the assumed constitutive relation: rate- and state-dependent governing laws and slip-dependent law.

# The June 2000 seismic sequence in the South Iceland Seismic Zone

The sequence started on June 17, at 15:40:41 UTC, with an event of magnitude  $M_S = 6.6$  (Pedersen *et al.*, 2001), with hypocenter located at (63.973 °N, 20.367 °W, 6.3 Km) (Stefansson *et al.*, 2003; Arnadóttir *et al.*, 2006).



- The largest events ( $M \sim 5$ ) occurring in the first five minutes are:

8s, 26s, 30 s, 130s, 226s

- In intermediate–far field:

26s, 30 s, 226s

- Reasonably are not secondary aftershocks:

26s, 30 s.

- The 30 s event is affected by the mainshock and also by the 26 s aftershock.

# The numerical approach

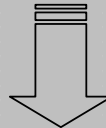
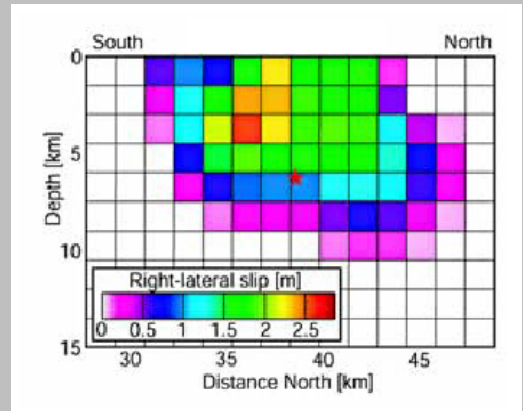
For the June 17 2000 mainshock we assume:

1) The slip distribution retrieved by a joint inversion of GPS and InSAR data (*Arnadottir et al., 2003*) →

2) A bilateral Haskell model, with a rupture velocity  $v_r = 2500$  m/s

3) A Bouchon ramp source time function (*Bouchon, 1981*) with a rise time  $t_0$  equal to 1.6 s

4)  $7^\circ$ ,  $88^\circ$  and  $180^\circ$  for the strike, the dip and the rake angles, respectively (i. e. right-lateral strike slip mechanism), on the basis of the aftershock distribution (*Stefansson et al., 2003*)



Using the discrete wavenumber and reflectivity code developed by *Cotton and Coutant (1997)* we compute the resulting stress field variations  $\Delta\sigma_{ij}(\mathbf{x}, t)$

The values of the tensor  $\Delta\sigma_{ij}$  are calculated on the 26 s fault plane up to 2.78 Hz, in a total of  $12 \times 8$  “receivers”, located in nodes uniformly spaced 1650 m in the strike direction and at depths of 0 m, 1650 m, 3300 m, 4950 m, 6550 m, 8100 m, 9900 m and 11550 m.

The spatial sampling of the receiver grid is not sufficient to correctly resolve the dynamic processes occurring during the rupture nucleation and propagation (*Bizzarri and Cocco, 2003; 2005*), as well as the temporal discretization.

We develop an algorithm that employs a  $\mathcal{C}^2$  cubic spline to interpolate  $\Delta\sigma_{ij}$  in space and in time.



In the numerical code presented by *Bizzarri and Cocco (2005)* at time  $t$  and in each fault node, the dynamic load is:  $\mathcal{L}_i = \mathbf{f}_{ri} + T_{0i} + \Delta\sigma_{2i}$  ( $i = 1$  and  $3$ ).

$T_{0i}$  are the components of the initial traction ( $\mathbf{T}_0(x_1, x_3) = \tau_0(x_1, x_3)(\cos(\varphi_0), 0, \sin(\varphi_0))$ )

$\mathbf{f}_{ri}$  are the components of the load (namely the contribution of the restoring forces,  $\mathbf{f}_r$ ) exerted by the neighbouring points:

$$\mathbf{f}_{ri} = (M^- \mathbf{f}_i^+ - M^+ \mathbf{f}_i^-) / (M^+ + M^-),$$

where  $M^+$  and  $M^-$  are the masses of the “+” and “-” half split-node of the fault plane  $\Sigma$  and  $\mathbf{f}^+$  is the force acting on partial node “+” caused by deformation of neighbouring elements located in the “-” side of  $S$  (and viceversa for  $\mathbf{f}^-$ ).

$\{\Delta\sigma_{2i}\}$  are coupled to the components of the fault friction  $T_i$  via

$$\begin{aligned} \frac{d^2}{dt^2} u_1 &= \alpha [\mathcal{L}_1 - T_1] \\ \frac{d^2}{dt^2} u_3 &= \alpha [\mathcal{L}_3 - T_3] \end{aligned}$$

where  $\alpha \equiv \mathcal{A} ((1/M^+) + (1/M^-))$ ,  $\mathcal{A} = \Delta x_1 \Delta x_3$ .  $T_i$  express on the governing law.

# Observational constraints

1) Perturbed rupture time  $t_r = 25.9 \pm 0.1$  s

2) Hypocenter ( $63.951 \pm 0.004$  °N,  $21.689 \pm 0.008$  °W,  $8.9 \pm 1.3$  Km)  $\leftrightarrow$  on fault coordinates of ( $16500 \pm 450$ ,  $8900 \pm 1300$ ) m (*Antonioli et al., 2006*)

3') From the aftershocks distribution shown in *Hjaltadottir and Vogfjord (2005)* we consider the seismic part of the fault (*A*) limited in latitude between  $63.890$  °N and  $63.947$  °N (in the case of North–South fault this corresponds to  $[9700, 16050]$  m in strike direction) and limited in depth between  $5400$  m and  $8100$  m

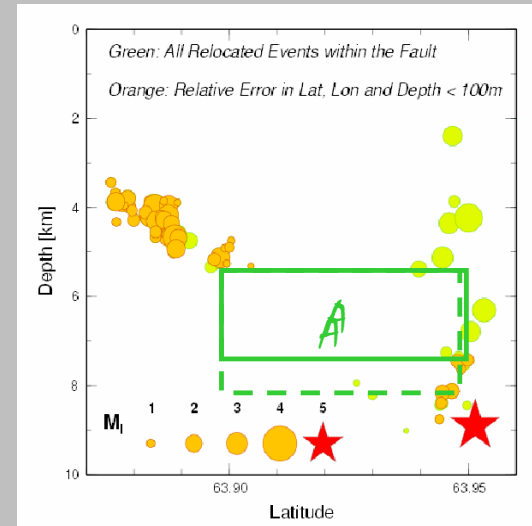


Upper bound estimates':

$$M_0 = 1.23 \times 10^{15} A^{3/2} = 8.73 \times 10^{16} \text{ Nm};$$

$$\text{Av. fault slip: } \langle u \rangle_A = M_0 / (\rho v_S^2 A) = 0.14 \text{ m};$$

$$\text{Av. stress drop: } \langle \Delta \tau \rangle_A = 2M_0 / (\pi W_A L_A) = 1.62 \text{ MPa}$$



4)  $M_w \geq 5$  (*Arnadottir et al., 2006; Vogfjord, 2003*)  $\Rightarrow M_0 \cong 3.2 \times 10^{16}$  Nm

# 3-D Results with DR law – homogeneous

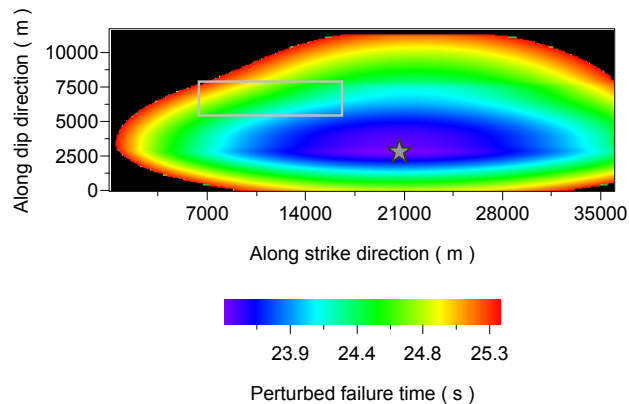
## Dieterich – Ruina governing law

$$\tau = \mu(v, \Psi) \sigma_n^{eff} = \left[ \mu_* + a \ln\left(\frac{v}{v_*}\right) + b \ln\left(\frac{\Psi v_*}{L}\right) \right] \sigma_n^{eff}$$

$$\frac{d}{dt} \Psi = 1 - \frac{\Psi v}{L}$$

Can be neglected (see Antoniolli et al., 2006)

$\sigma_n^{eff} = 2.5$  MPa everywhere; acting only  $\Delta\sigma_{21}$



## Perturbed rupture times

$$v(x_1, x_3, t) \geq v_l \Rightarrow t_p(x_1, x_3) = t$$

$v_l = 0.1$  m/s, in agreement with Belardinelli et al. (2003); Antoniolli et al. (2005); Rubin and Ampuero (2005); Ziv and Cochard (2006)

$t_p^{min} = 23.47$  s @ (20700, 2900) m

$M_0 = 2.37 \times 10^{19}$  Nm

Whole fault

From Bizzarri and Belardinelli (Nov. 2006; subm. to JGR)



# 3-D Results with DR law – homogeneous

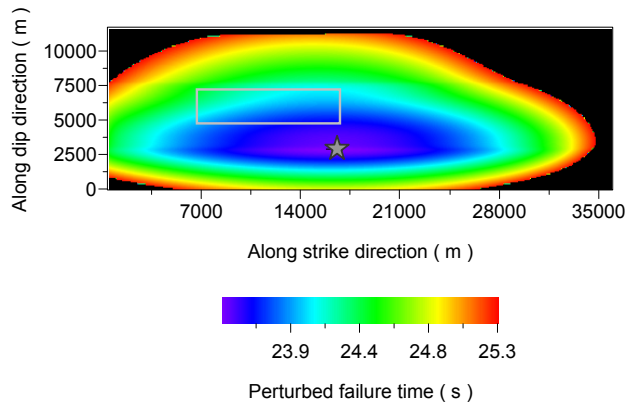
## Dieterich – Ruina governing law

$$\tau = \mu(v, \Psi) \sigma_n^{eff} = \left[ \mu_* + a \ln\left(\frac{v}{v_*}\right) + b \ln\left(\frac{\Psi v_*}{L}\right) \right] \sigma_n^{eff}$$

$$\frac{d}{dt} \Psi = 1 - \frac{\Psi v}{L}$$

Can be neglected (see Antoniolli et al., 2006)

$\sigma_n^{eff} = 2.5$  MPa everywhere; acting also  $\Delta\sigma_{22}$



## Perturbed rupture times

$$v(x_1, x_3, t) \geq v_l \Rightarrow t_p(x_1, x_3) = t$$

$v_l = 0.1$  m/s, in agreement with Belardinelli et al. (2003); Antoniolli et al. (2006); Rubin and Ampuero (2005); Ziv and Cochard (2006)

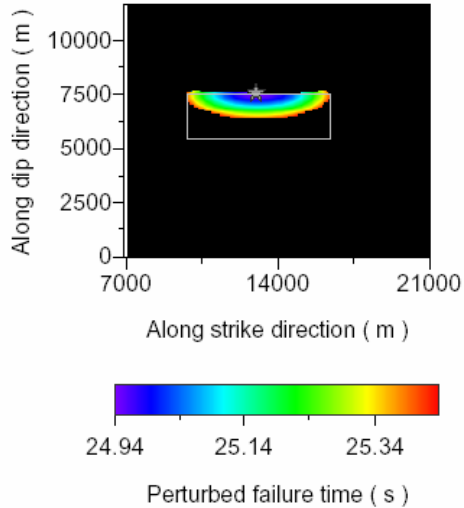
$t_p^{min} = 23.47$  s @ (16500, 2900) m

$M_0 = 2.23 \times 10^{19}$  Nm

Whole fault

From Bizzarri and Belardinelli (Nov. 2006; subm. to JGR)

# 3-D Results with DR law – heterogeneous



Effective normal stress profile



Velocity strengthening behavior ( $a > b$ ) for  $x_1 < 9700$  m,  $x_1 > 16500$  m,  $x_3 > 8800$  m

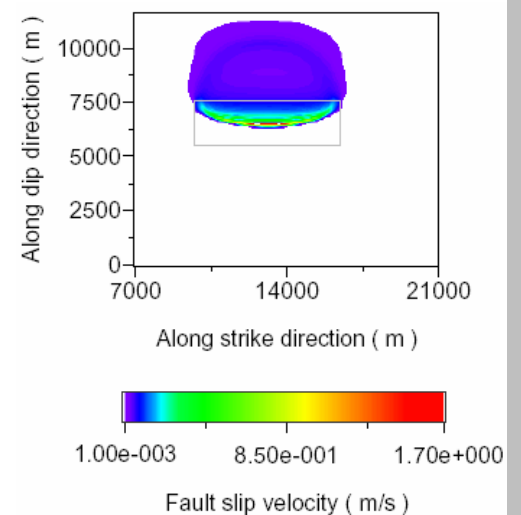
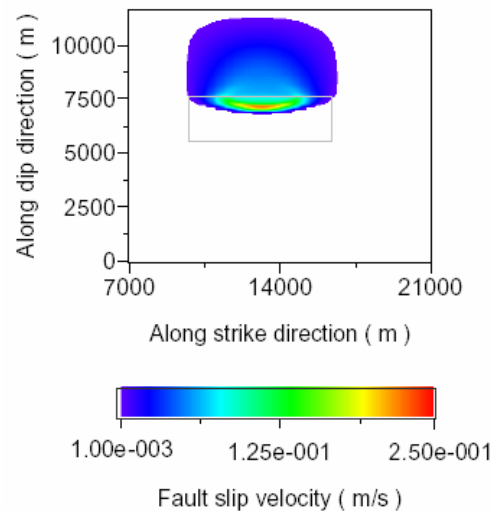
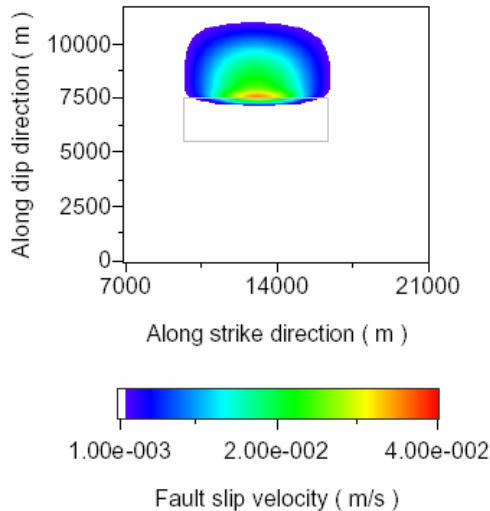
$t_p^{min} = 24.94$  s @ (13200, 7500) m

$M_0 = 2.27 \times 10^{16}$  Nm

[9700, 16500] m in strike direction

[6400, 7500] m in dip direction

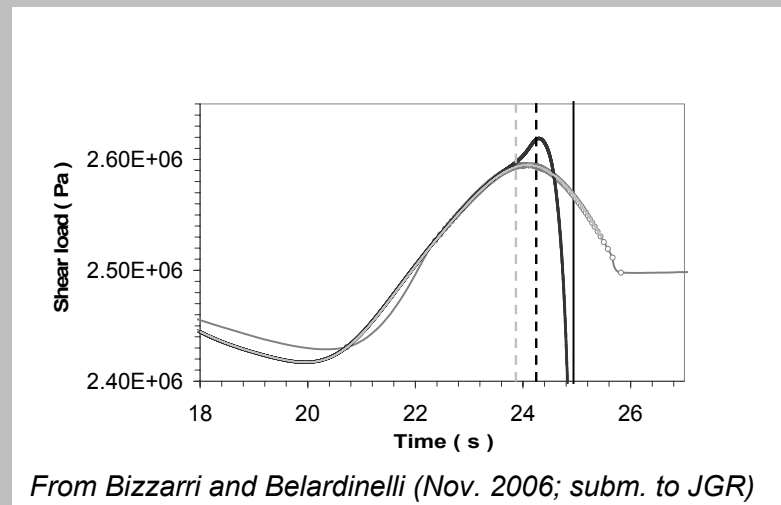
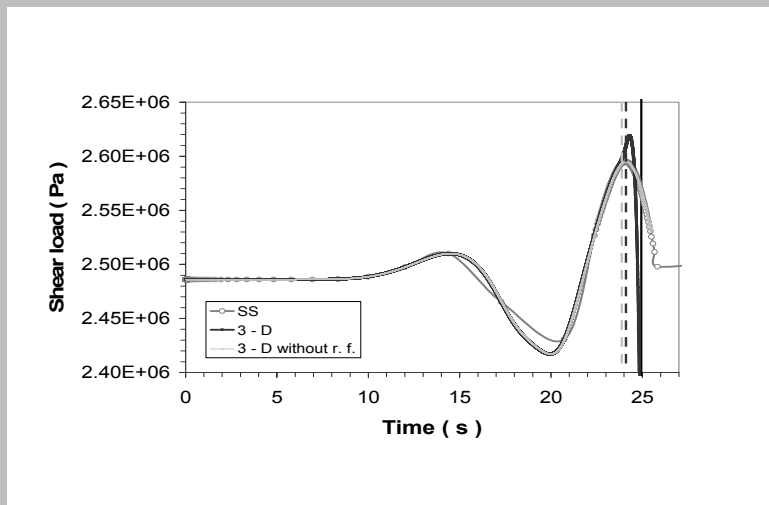
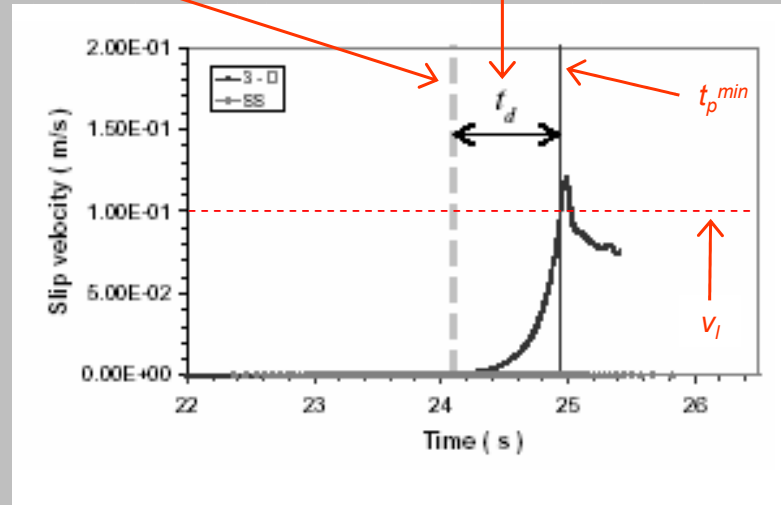
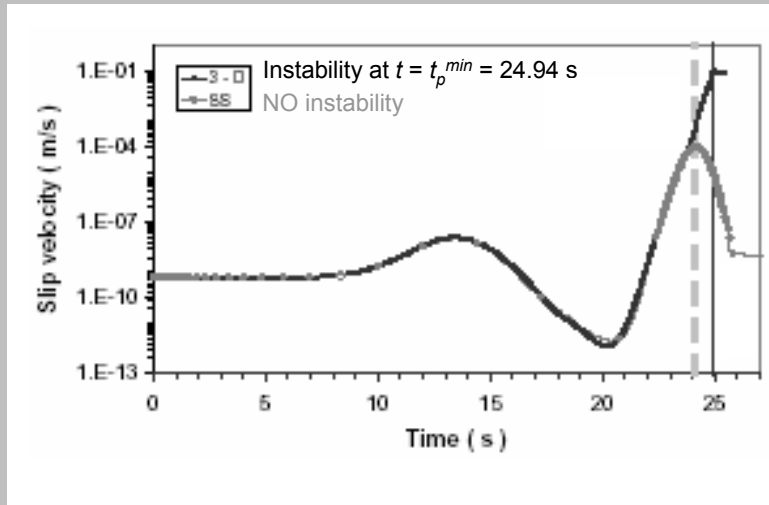
From Bizzarri and Belardinelli (Nov. 2006; *subm. to JGR*)





Peak in shear perturbing stress

Triggering delay



From Bizzarri and Belardinelli (Nov. 2006; subm. to JGR)

# 3-D Results with RD law – heterogeneous

## Ruina – Dieterich governing law

$$\tau = \left[ \mu_* + a \ln\left(\frac{v}{v_*}\right) + b \ln\left(\frac{\Psi v_*}{L}\right) \right] \sigma_n^{eff}$$

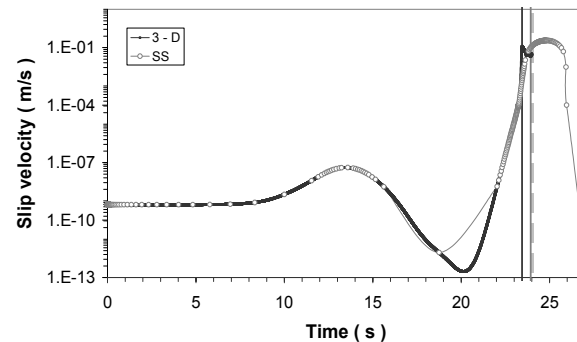
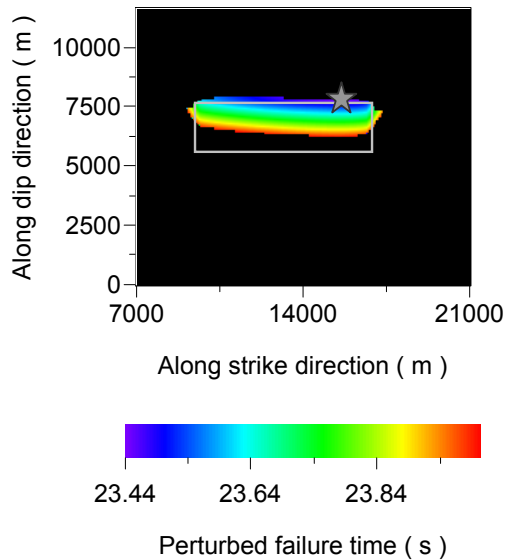
$$\frac{d}{dt} \Psi = -\frac{\Psi v}{L} \ln\left(\frac{\Psi v}{L}\right) \quad \text{Can be neglected}$$

$t_p^{min} = 23.44 \text{ s @ } (15700, 7900) \text{ m}$

$M_0 = 2.02 \times 10^{16} \text{ Nm}$

[9000, 17300] m in strike direction

[6300, 8000] m in dip direction

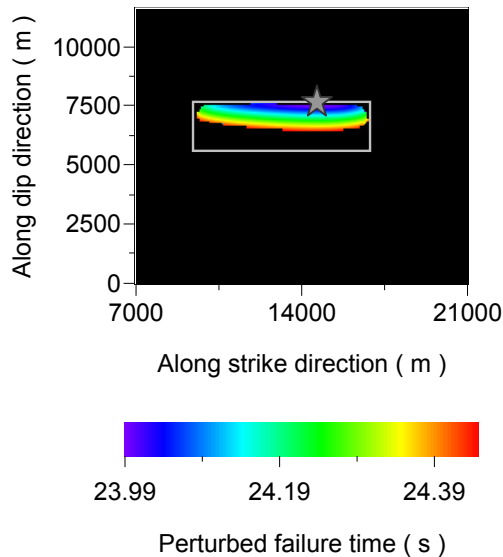


From Bizzarri and Belardinelli (Nov. 2006; *subm. to JGR*)

# Different values of $L$ in the RD law

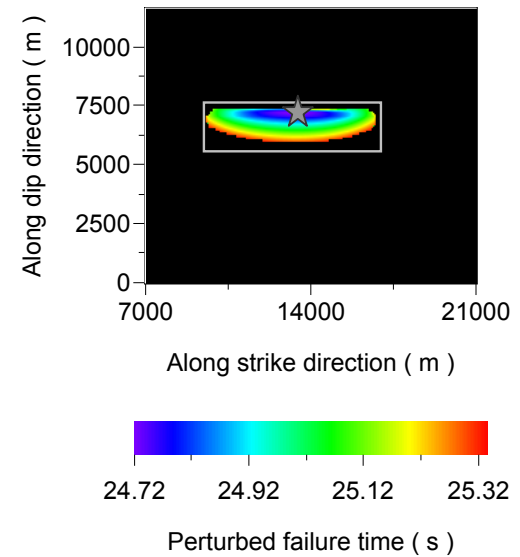
$L = 5$  mm

$t_p^{min} = 23.99$  s @ (14600, 7600) m  
 $M_0 = 1.27 \times 10^{16}$  Nm  
 [9500, 16800] m in strike direction  
 [6500, 7700] m in dip direction



$L = 10$  mm

$t_p^{min} = 24.72$  s @ (13300, 7300) m  
 $M_0 = 2.17 \times 10^{16}$  Nm  
 [9500, 16700] m in strike direction  
 [6000, 7400] m in dip direction



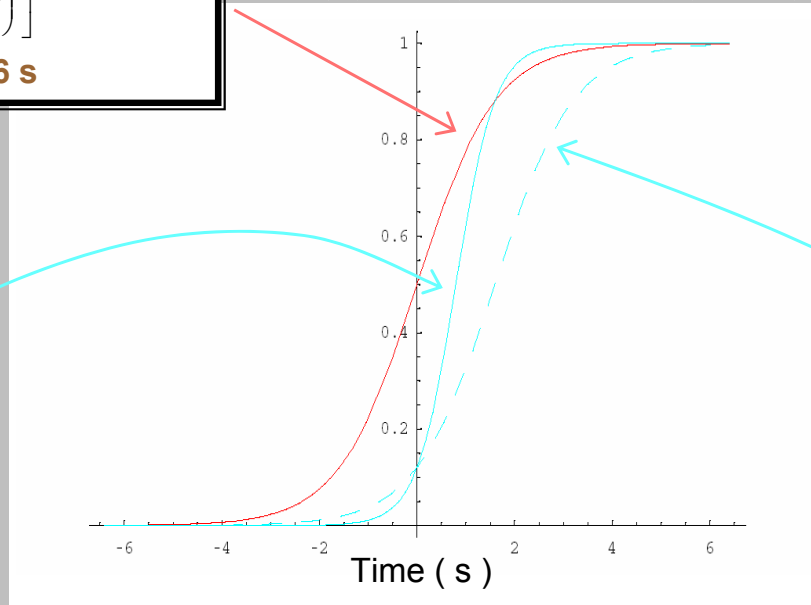
From Bizzarri and  
 Belardinelli (Nov.  
 2006; *subm. to JGR*)

# Alternative source time functions #1

Bouchon source time function:

$$f(t) = \frac{1}{2} \left[ 1 + \tanh\left(\frac{t}{t_0}\right) \right]$$

Bouchon, 1981;  $t_0 = 1.6$  s



Modified Bouchon source time function:

$$f(t) = \frac{1}{2} \left[ 1 + \tanh\left(\frac{t - \frac{t_0}{2}}{\frac{t_0}{2}}\right) \right]$$

corrected from *Cotton and Campillo, 1995*;  
 $t_0 = 1.6$  s. Increased amplitudes in  $\Delta\sigma_{21}$  peaks.

Modified Bouchon source time function:

$$f(t) = \frac{1}{2} \left[ 1 + \tanh\left(\frac{t - \frac{t_0}{2}}{\frac{t_0}{2}}\right) \right]$$

corrected from *Cotton and Campillo, 1995*;  
 $t_0 = 3.2$  s. Only a temporal shift.

# 3-D Alternative source time functions #2

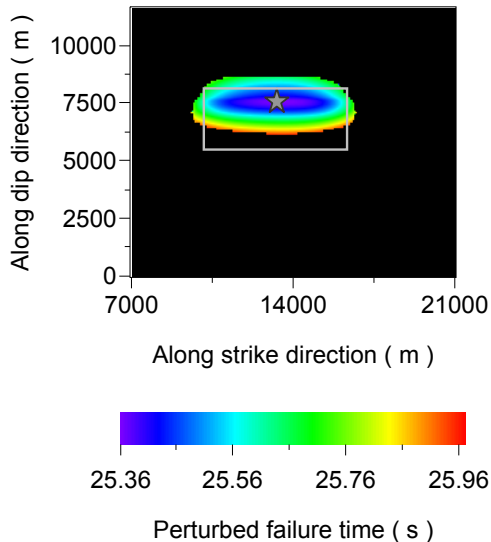
Modified Bouchon,  $t_0 = 1.6$  s;  
 $\sigma_n^{eff*} = 4.2$  MPa – DR law

$t_p^{min} = 25.36$  s @ (13500, 7600) m

$M_0 = 2.59 \times 10^{16}$  Nm

[9500, 16700] m in strike direction

[6200, 8700] m in dip direction



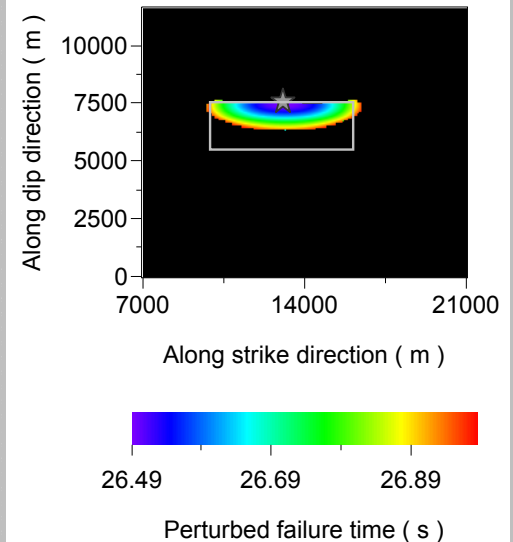
Modified Bouchon,  $t_0 = 3.2$  s  
DR law

$t_p^{min} = 26.49$  s @ (13000, 7500) m

$M_0 = 2.30 \times 10^{16}$  Nm

[9700, 16500] m in strike direction

[6400, 7600] m in dip direction



# Conclusions

- ✓ We simulate the remote triggering in a *truly* 3–D fault model with different governing laws;
- ✓ We generalize the results of *Antonioli et al. (2006)*, providing additional details of the 26 s event: the location of the hypocenter, its failure time, the rupture area and the seismic moment;
- ✓ The effective normal stress and the pre–stress are heterogeneous;
- ✓ The spring–slider and the 3–D model are intrinsically different, but we observe an excellent agreement during the slow nucleation phase...
- ✓ ... during the acceleration, in the 3–D model the dynamic load of the slipping points further decrease the perturbed failure time;

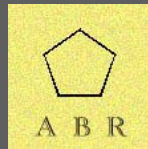


- ✓ The agreement with observations increases considering a modified (and more causal) source time function;
- ✓ If detailed informations of the initial state of the fault, potentially highly heterogeneous, were available the agreement with observations will be even better.

<i>Case</i>	<i>Constitutive law</i>	<i>Rupture extension along strike (m)</i>	<i>Rupture extension along dip (m)</i>	<i>Hypocenter location (m)</i>	<i>Origin time (s)</i>	<i>Total seismic moment <math>M_0</math> (Nm)</i>
F	DR	[9700, 16500]	[6400, 7500]	(13200,7500)	24.94	$2.27 \times 10^{16}$
L	RD ( $L = 10$ mm)	[9500, 16700]	[6000, 7400]	(13300,7300)	24.72	$2.17 \times 10^{16}$
O	DR	[9700, 16500]	[6400, 7600]	(13000,7500)	26.49	$2.30 \times 10^{16}$
P	DR	[9500, 16700]	[6200, 8700]	(13500,7600)	25.36	$2.59 \times 10^{16}$
<b><i>Observational constraints</i></b>		<b>[9700, 16500]</b>	<b>[5400, 7400]</b>	<b>(16500 ± 450, 8900 ± 1300)</b>	<b>25.9 ± 0.1</b>	<b><math>\cong 3.2 \times 10^{16}</math></b>

**Thank you!**

**This slide is empty intentionally.**



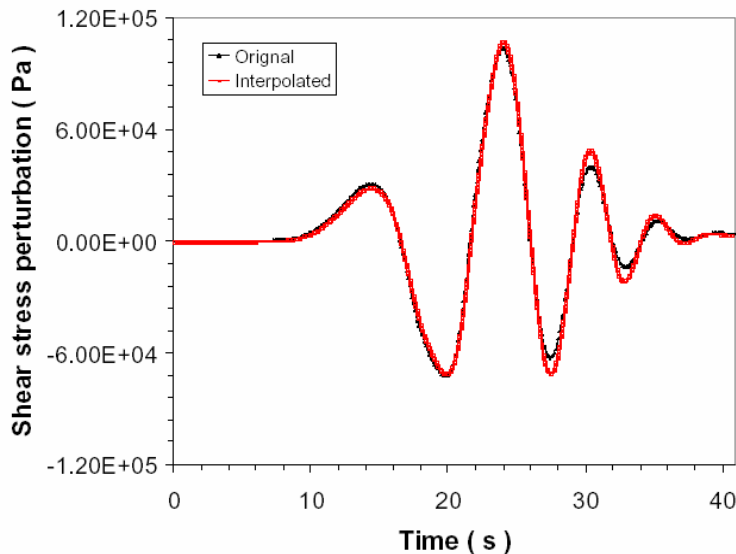
# **Support Slides: Parameters, Notes, etc.**

*To not be displayed directly. Referenced above.*

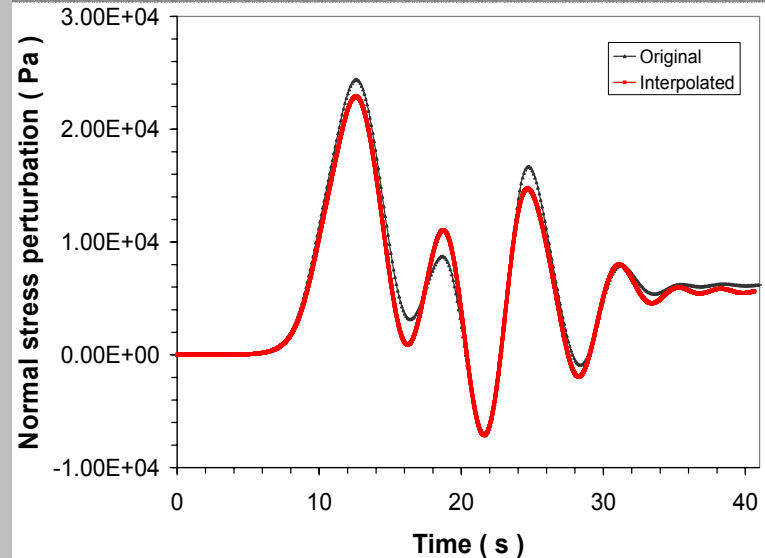
The spatial sampling of the receiver grid is not sufficient to correctly resolve the dynamic processes occurring during the rupture nucleation and propagation (*Bizzarri and Cocco, 2003; 2005*), as well as the temporal discretization.

We develop an algorithm that employs a  $\mathcal{C}^2$  cubic spline to interpolate  $\Delta\sigma_{ij}$  in space and in time.

In the hypocenter at  $t = 26.37$  s



In the hypocenter at  $t = 26.37$  s



<i>Parameter</i>	<i>Value</i>
$\mathcal{D}$	parallelepiped that extends $x_{1_{end}} = 36.5$ Km along $x_1$ , $x_{2_{end}} = 10$ Km along $x_2$ and $x_{3_{end}} = 11.6$ Km along $x_3$
$\Sigma = \mathcal{O}\mathcal{S}$	$\{ \mathbf{x} \mid x_2 = x_2^J = 5000 \text{ m} \}$
$\Delta x_1 = \Delta x_2 = \Delta x_3 \equiv \Delta x$	100 m (a)
Number of nodes	4,289,571
$\Delta t$	$1.27 \times 10^{-3}$ s (a)
Number of time levels	33,650
$v_l$	0.1 m/s
$\sigma_n^{eff*}$	2.5 MPa
$\varphi(x_1, x_3, 0)$	$\varphi_0 = 180^\circ$
$v(x_1, x_3, 0)$	$v_{init} = 6.34 \times 10^{-10}$ m/s (= 20 mm/yr)
$\Psi(x_1, x_3, 0)$	$\Psi^{ss}(v_{init}) = 1.577 \times 10^6$ s ( $\cong 18.25$ d)
$\sigma_n^{eff}(x_1, x_3, 0)$	See Table 3
$\tau_0(x_1, x_3)$	$\mu^{ss}(v_{init})\sigma_n^{eff}(x_1, x_3, 0)$
$a$	0.003 (b)
$b$	0.010
$L$	$1 \times 10^{-3}$ m
$\mu_*$	0.7
$v_*$	$v_{init}$
$\alpha_{LD}$	0

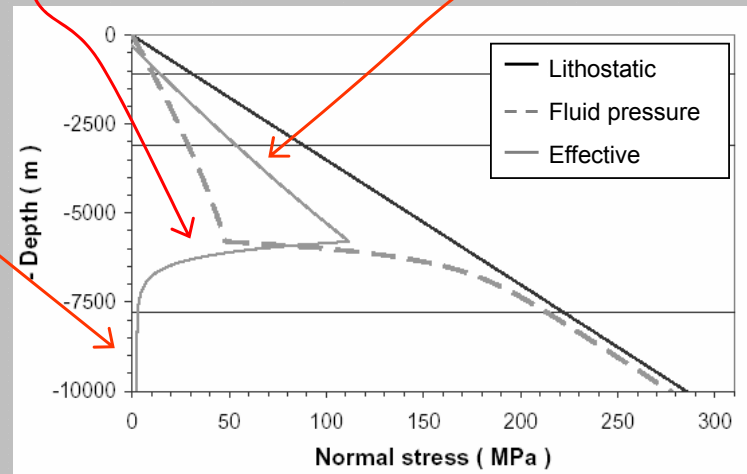
Crustal profile (from *Vogfjord et al., 2002; Antonioli et al., 2006*)

<i>Layer # k</i>	$v_{P_k}$ (m/s)	$v_{S_k}$ (m/s)	$\rho_{rock_k}$ (Kg/m <sup>3</sup> )	<i>Up to depth of <math>x_{3_k}</math> (m)</i>
1	3200	1810	2300	1100
2	4500	2540	2540	3100
3	6220	3520	3050	7800
4	6750	3800	3100	11600

$$\sigma_{n_0}^{eff}(x_3) \equiv \sigma_n^{eff}(x_1, x_3, t) =$$

$$\left\{ \begin{array}{l} \hat{p}^{(litho)}(x_3) - \Delta\sigma^{(dev)} - p_{fluid}^{(hydro)}(x_3) \\ \hat{p}^{(litho)}(x_3) - \Delta\sigma^{(dev)} - \left[ \hat{p}^{(litho)}(x_3) - \Delta\sigma^{(dev)} - \sigma_n^{eff*} \right. \\ \left. - \Delta P_2 e^{-\frac{x_3 - x_3^*}{h^*}} + \sigma_n^{eff*} e^{-\frac{x_3 - x_3^*}{h^*}} \right] \\ \sigma_n^{eff*} = 2.5 \text{ MPa} \end{array} \right. \quad \begin{array}{l} , x_3 \leq x_3^* = 5800 \text{ m} \\ , x_3^* < x_3 < x_3^* + D^* \\ , x_3 \geq x_3^* + D^* = 8800 \text{ m} \end{array}$$

$$\Delta P_2 \equiv \hat{p}^{(litho)}(x_3^*) - \Delta\sigma^{(dev)} - p_{fluid}^{(hydro)}(x_3^*)$$



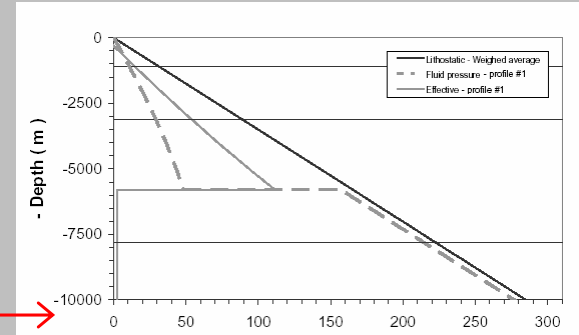


# **Support Slides 2: Parameters, Notes, etc.**

*To not be displayed directly. For discussion only.*

# Initial effective normal stress

Profile #	$\sigma_{n_0}^{eff}(x_3) \equiv \sigma_n^{eff}(x_1, x_3, t) =$
1	$\begin{cases} \hat{p}^{(litho)}(x_3) - \Delta\sigma^{(dev)} - p_{fluid}^{(hydro)}(x_3) & , x_3 \leq x_3^* \\ \sigma_n^{eff^*} & , x_3 > x_3^* = 5800 \text{ m} \end{cases}$



# Initial effective normal stress

<b>Profile #</b>	$\sigma_{n_0}^{eff}(x_3) \equiv \sigma_n^{eff}(x_1, x_3, t) =$
------------------	--

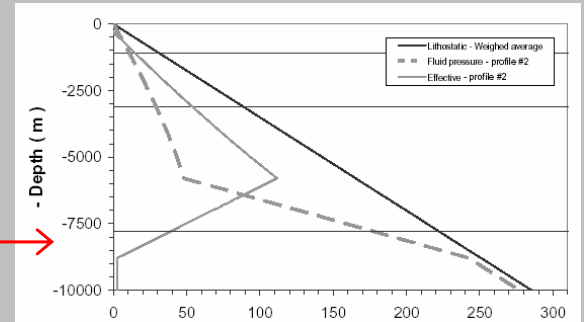
  

2

$$\sigma_n^{eff*} = \begin{cases} \hat{p}^{(litho)}(x_3) - \Delta\sigma^{(dev)} - p_{fluid}^{(hydro)}(x_3) & , x_3 \leq x_3^* \\ \hat{p}^{(litho)}(x_3) - \Delta\sigma^{(dev)} - \left[ \hat{p}^{(litho)}(x_3^*) - \Delta\sigma^{(dev)} - \sigma_n^{eff*} + \Delta P_2 \frac{(x_3 - x_3^* - D^*)}{D^*} - \sigma_n^{eff*} \frac{(x_3 - x_3^* - D^*)}{D^*} \right] & , x_3^* < x_3 < x_3^* + D^* \\ \sigma_n^{eff*} & , x_3 \geq x_3^* + D^* = 8800 \text{ m} \end{cases}$$

where:

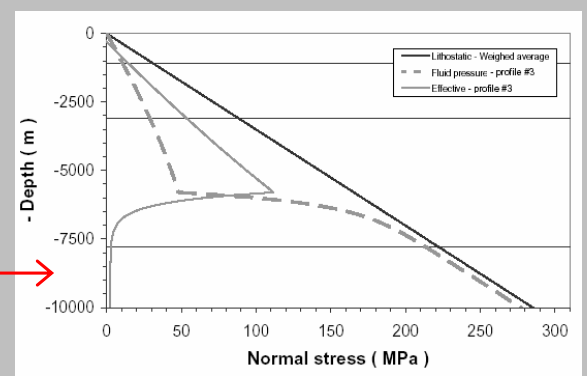
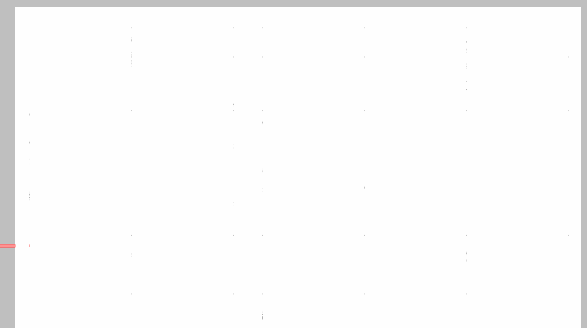
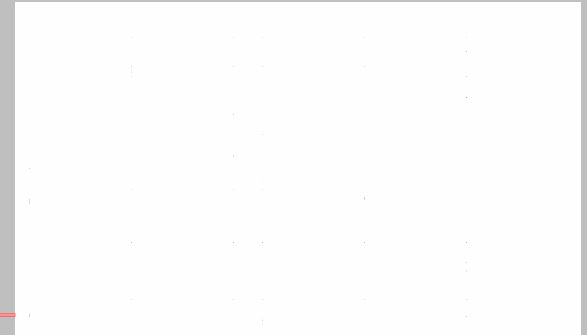
$$\Delta P_2 \equiv \hat{p}^{(litho)}(x_3^*) - \Delta\sigma^{(dev)} - p_{fluid}^{(hydro)}(x_3^*)$$



# Initial effective normal stress

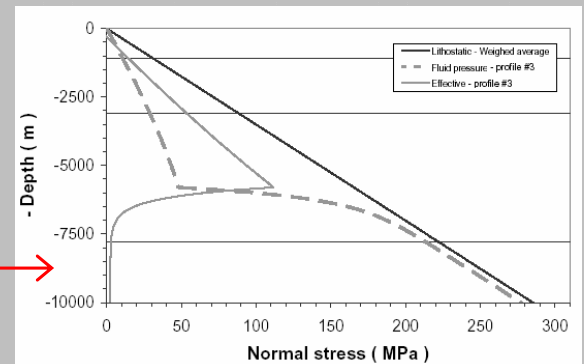
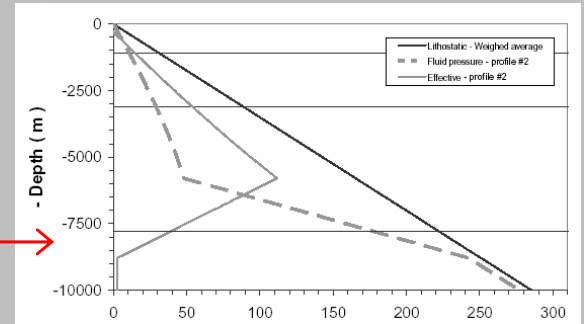
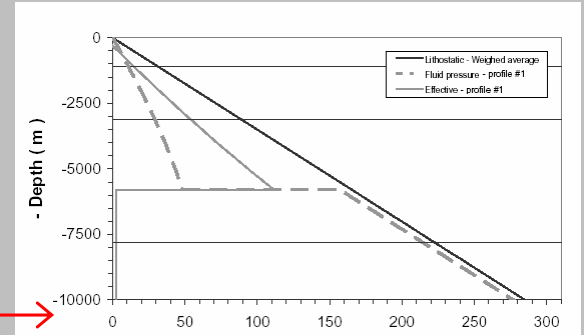
<b>Profile #</b>	$\sigma_{n_0}^{eff}(x_3) \equiv \sigma_n^{eff}(x_1, x_3, t) =$
------------------	--

3	$\left\{ \begin{array}{ll} \hat{p}^{(litho)}(x_3) - \Delta\sigma^{(dev)} - P_{fluid}^{(hydro)}(x_3) & , x_3 \leq x_3^* \\ \hat{p}^{(litho)}(x_3) - \Delta\sigma^{(dev)} - \left[ \hat{p}^{(litho)}(x_3) - \Delta\sigma^{(dev)} - \sigma_n^{eff*} - \Delta P_2 e^{-\frac{x_3 - x_3^*}{h}} + \sigma_n^{eff*} e^{-\frac{x_3 - x_3^*}{h}} \right] & , x_3^* < x_3 < x_3^* + D^* \\ \sigma_n^{eff*} & , x_3 \geq x_3^* + D^* \end{array} \right.$
---	--



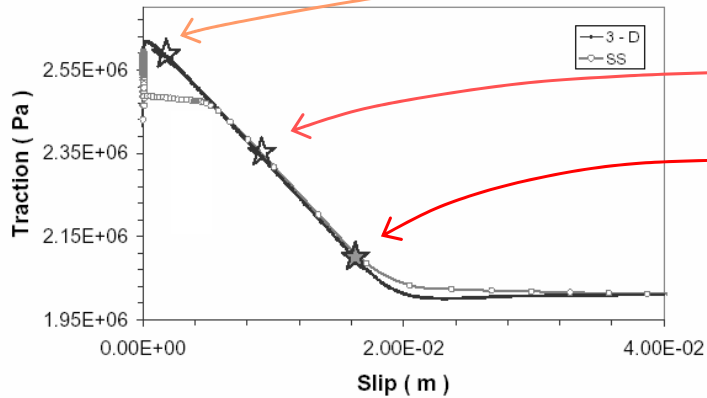
# Initial effective normal stress

Profile #	$\sigma_{n_0}^{eff}(x_3) \equiv \sigma_n^{eff}(x_1, x_3, t) =$
1	$\begin{cases} \hat{p}^{(litho)}(x_3) - \Delta\sigma^{(dev)} - p_{fluid}^{(hydro)}(x_3) & , x_3 \leq x_3^* \\ \sigma_n^{eff*} & , x_3 > x_3^* = 5800 \text{ m} \end{cases}$
2	$\begin{cases} \hat{p}^{(litho)}(x_3) - \Delta\sigma^{(dev)} - p_{fluid}^{(hydro)}(x_3) & , x_3 \leq x_3^* \\ \hat{p}^{(litho)}(x_3) - \Delta\sigma^{(dev)} - \left[ \hat{p}^{(litho)}(x_3) - \Delta\sigma^{(dev)} - \sigma_n^{eff*} + \Delta P_2 \frac{(x_3 - x_3^* - D^*)}{D^*} - \sigma_n^{eff*} \frac{(x_3 - x_3^* - D^*)}{D^*} \right] & , x_3^* < x_3 < x_3^* + D^* \\ \sigma_n^{eff*} & , x_3 \geq x_3^* + D^* = 8800 \text{ m} \end{cases}$ <p>where:</p> $\Delta P_2 \equiv \hat{p}^{(litho)}(x_3^*) - \Delta\sigma^{(dev)} - p_{fluid}^{(hydro)}(x_3^*)$
3	$\begin{cases} \hat{p}^{(litho)}(x_3) - \Delta\sigma^{(dev)} - p_{fluid}^{(hydro)}(x_3) & , x_3 \leq x_3^* \\ \hat{p}^{(litho)}(x_3) - \Delta\sigma^{(dev)} - \left[ \hat{p}^{(litho)}(x_3) - \Delta\sigma^{(dev)} - \sigma_n^{eff*} - \Delta P_2 e^{-\frac{x_3 - x_3^*}{h}} + \sigma_n^{eff*} e^{-\frac{x_3 - x_3^*}{h}} \right] & , x_3^* < x_3 < x_3^* + D^* \\ \sigma_n^{eff*} & , x_3 \geq x_3^* + D^* \end{cases}$



# Effect of different $v_l$

## Dieterich – Ruina governing law



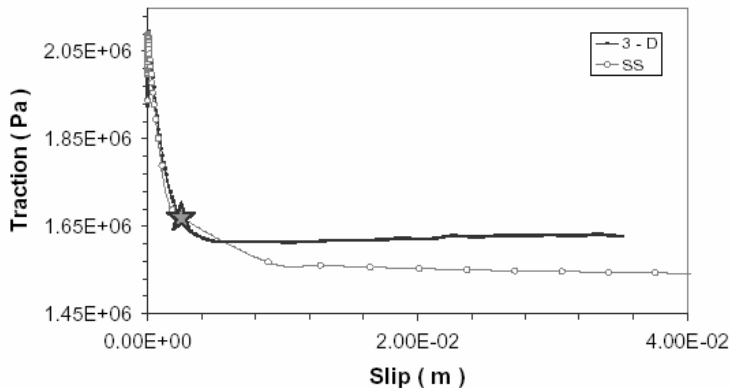
$v^H = 0.01 \text{ m/s } ( t = 24.56 \text{ s } )$

$v^H = 0.05 \text{ m/s } ( t = 24.84 \text{ s } )$

$v^H = v_l = 0.1 \text{ m/s } ( t = t_p = 24.94 \text{ s } )$

Failure occurs before traction reaches the residual level.

## Ruina – Dieterich governing law



From Bizzarri and Belardinelli (Nov. 2005; subm. to JGR)